Progress In Electromagnetics Research B, Vol. 57, 139–155, 2014

PN Code Acquisition Using Smart Antenna and Adaptive Thresholding CFAR Based on Ordered Data Variability for CDMA Communications

Kamel Berbra[1], Mourad Barkat[2,*], and Abderrahmane Anou[1]

Abstract—Recently, a novel approach for PN code acquisition of direct sequence code division multiple-access (DS-CDMA) systems in Rayleigh fading multipath channel was proposed in [1]. The authors considered a combination of adaptive thresholding constant false alarm rate (CFAR) and smart antennas to increase the system capacity and consequently enhance the detection performance. This paper considers still the problem of PN code acquisition for DS-CDMA communication systems over Rayleigh fading channels under the presence of multipath and multiple-access interference (MAI) signals. We propose and analyze an adaptive array acquisition system, which integrates an adaptive thresholding technique based on ordered data variability (ODV) index constant false alarm rate (ODV-CFAR) and digital beamforming where a low complexity least mean square (LMS) algorithm is used to calculate the optimal weighting coefficients. This approach is expected to mitigate interferences caused by the presence of multiple access interference and multipath. Unlike other approaches based on a fixed censoring point when the number of interferences is assumed known, ODV-CFAR processing does not require prior knowledge about the number of interferences. The simulation results show a robust performance of the proposed system in varying mobile communication channels.

1. INTRODUCTION

In direct sequence code division multiple access (DS-CDMA) communication systems, spectral expansion is achieved by modulating each unit of information to be transmitted with a pseudo-noise (PN) random-like code sequence, where each pulse is denominated as a chip. At the receiver the demodulation is performed by multiplying the received signal by an aligned replica of the code used in the transmitter. The alignment condition is essential for a successful demodulation since only when the codes are perfectly aligned the received signal is reverted to its original format. The alignment operation known as code synchronization is usually carried out in two steps; an initial coarse synchronization process known as a code acquisition followed by a fine synchronization process known as code tracking. Acquisition is the process of searching through an uncertainty region of code phases until the correct phase is found. The uncertainty region is divided into a number of cells where a cell may be as small as a fraction of a PN chip interval. In serial acquisition, the received signal is correlated with a locally generated replica of the transmitted code and the correlation value is compared to a threshold in order to make a decision about synchronization [2].

The setting of the threshold plays an important role on the performance of the acquisition process and is the most challenging task. A lot of research on PN code acquisition has been carried out, but focused on fixed–threshold acquisition where the threshold value is selected for a specific radio environment. This results in a high false alarm rate and/or low probability of detection [3–6]. Since the power of the received signals in mobile communication decreases with distance and are also subject

Received 24 September 2013, Accepted 4 December 2013, Scheduled 4 December 2013

* Corresponding author: Mourad Barkat (mbarkat58@gmail.com).

[1] Department of Electronics, University of Saad-Dahlab-Blida, Algeria. [2] Department of Electrical and Computer Engineering Technology, Valencia College, Orlando, Florida 32811, USA.

to fast fading and slowly varying mean signal strength, fixed threshold detection schemes are unable to adapt to these radio varying environments. One of the most promising approaches to meet these challenges is the use of adaptive thresholding techniques. The goal of these approaches is to improve the acquisition performance by keeping a constant probability of false alarm (P_{fa}) [7]. Adaptive thresholding CFAR processing is well developed in automatic radar signal detection [8].

In conventional wireless communications, a single antenna is used at the receiver. Such systems are vulnerable to multipath and multiple access interference (MAI) caused by other users. Since in practice the codes are not perfectly orthogonal, while the MAI caused by any one user is generally small, as the number of interferences or their power increases, MAI becomes substantial. In CDMA systems, MAI is the major factor limiting the performance and hence, limits the number of supported users to share the same channel known also as the capacity of the system. The effect of the multiple access interference, distinctive of CDMA systems, also has to be incorporated in the analysis of code acquisition. Therefore, analysis of the effect of MAI on the system performance as well as ways to suppress MAI has been the major focus of recent research on CDMA. A large amount of the research has focused on developing these theories to address the difficulties of wireless communication. A number of different techniques have been developed in this field. Many techniques are used to mitigate this effect as shown in some very recent papers [9, 10]; the work in [9] compares maximal length sequences (m-sequences) codes and Gold sequences codes in order to select a spreading sequence possessing desirable characteristics which would minimize the effect of multiple access interference for implementation in CDMA systems. A blind paralind multiuser detection over multipath fading channels to further suppress MAIs in CDMA systems has been proposed and analyzed in [10]. A possible solution to overcome these channel impairments is to use a smart antenna by steering beams toward the desired user while decreasing the total power level of multiuser access interference (MAI). The smart antennas can increase the capacity of CDMA systems through interference suppression by exploiting the spatial diversity [11]. In [13, 14] smart antennas have been considered for acquisition where a correlator was used in each antenna element and the outputs of the correlators were combined using a beamformer (BF). Smart antenna systems attract a lot of attentions now and believably more in the future, as they can increase the performance of mobile communication systems dramatically.

In [1], Sofwan and Barkat considered a novel approach using adaptive thresholding CFAR processing combined to smart antennas as a powerful method to improve the PN code acquisition performance. They used the trimmed-mean (TM) CFAR processor for adaptive thresholding [14]. The same acquisition system was adopted in [15], but using the censored mean level detector CMLD-CFAR [16] in a Rayleigh fading multipath channel. The above mentioned systems used adaptive order statistic detection based on a fixed censoring point and they perform robustly as long as the interferences are properly discarded. However, due to the lack of a *priori* knowledge about the radio environment, the censored cells may be poorly selected causing significant performance degradation [17]. Hence, to overcome the above mentioned problem, we propose in this paper the use of an automatic censoring acquisition processor based on ordered data variability index ODV-CFAR [18]. The censored cells are automatically determined according to the actual number of interferences and thus the adaptive threshold is set accordingly. We recall that automatic censoring was extensively used in the literature [19–24]. The proposed system which uses a combination of smart antennas and adaptive ODV-CFAR processing demonstrates a robust performance for PN code acquisition regardless of the surroundings as will be shown in the next coming sections.

The remainder of this paper is organized as follows. In Section 2, a description of the proposed PN code acquisition system and the problem formulation are presented. The automatic censoring processor considered with the performance analysis as well as the expression for the probability of false alarm are provided in Section 3. Monte Carlo simulation results and discussions are given in Section 4. The findings and conclusions are then discussed in Section 5. The mathematical derivations of statistics of the correlator output and probability of false alarm P_{fa} are given in the Appendices A and B respectively.

2. SYSTEM DESCRIPTION AND PROBLEM FORMULATION

The block diagram of the proposed serial search acquisition DS-CDMA system with smart antennas is shown in Figure 1. A linear array with M elements and spacing d equal to one half of the carrier

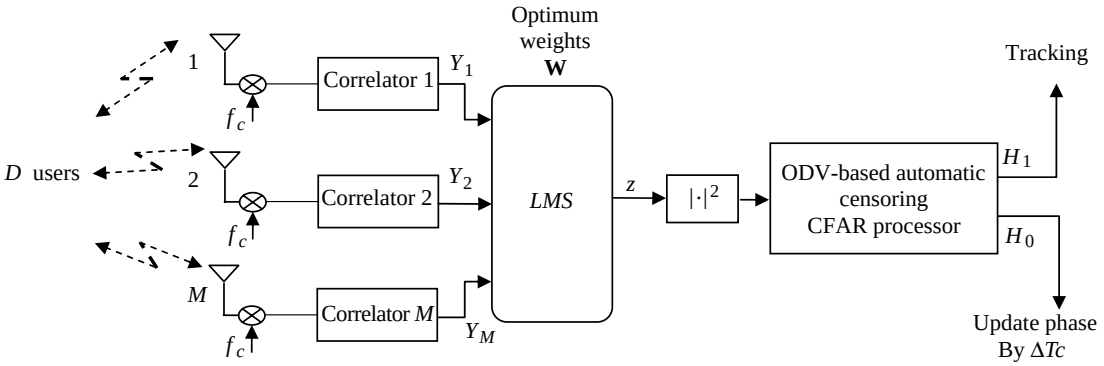

Figure 1. Block diagram of the proposed acquisition scheme with smart antennas.

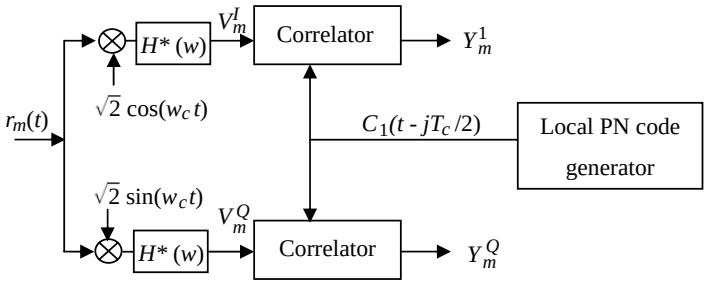

Figure 2. Correlator block diagram.

wavelength is assumed ($d = 0.5\lambda$), where λ is the wavelength of the carrier transmitted signal. The array antenna elements are also assumed to have an identical response to any direction.

In this reverse link, we assume that there are D actively transmitting users in the system; the first user is considered as the initial synchronization user whose performance is to be evaluated. Each user is assigned a unique CDMA code sequence $C_k(t)$ which spreads the data sequence while all the users transmit with orthogonal PN codes and their signals fade independently. In each branch Y_m of Figure 1, z represents a complex signal with the in-phase I and quadrature-phase Q components while $\mathbf{W} = [w_1\ w_2\ \ldots\ w_M]^T$ are the complex beam former weights and T denotes transpose.

The received signal is first down-converted into in-phase I and quadrature-phase Q components by using a matched filter to the rectangular shaping pulse of duration T_c to discard the carrier frequency at $2w_c$ as shown in Figure 2. Two I-Q correlators perform a correlation over an observation interval or dwell time interval $\tau_D = RT_c$ between the locally generated PN code $C_1(t-\Delta T_c)$ of the desired user and the received signals; in our case $\Delta = 0.5$. The LMS block is used to process the information obtained by the antenna array in order to optimize the complex weights, multiplying the incoming signals with the complex weights obtained and summing them together (spatial correlation) to obtain the desired radiation pattern. The optimization is based on minimizing the contribution from the interferences while producing maximum beam gain at the desired user direction. Then, the output of the LMS processor goes through an automatic censoring processor unit which is a CFAR based on ordered data variability index (ODV-CFAR) [18]. The proposed detector does not require any *a priori* information about the radio channel and uses the variability index statistic to reject the corrupted cells so that a threshold can then be set in order to decide as to whether there is acquisition or not.

2.1. Transmitted Signals and Channel Model

The complex transmitted signal for the kth user can be expressed as

$$S_k(t) = \sqrt{2P_k} b_k(t) C_k(t) e^{j(w_c t + \varphi_k)} \tag{1}$$

where

P_k is the transmitted power of the kth signal,
$b_k(t)$ is the data waveform,
$C_k(t)$ is the spreading sequence of the kth user,
w_c the common angular carrier frequency, and
φ_k the phase introduced by the kth modulator.

Assuming D users communicating over the same channel, the first one is the initial synchronization user whose PN code is being acquired (acquisition phase), while the others are the data transmission users who have finished acquisition. During the preamble-assisted acquisition phase, the transmitter aids the initial synchronization by transmitting an unmodulated PN sequence $b_1(t) = 1$.

Each signal $S_k(t)$, $k = 1, 2, \ldots, D$ is transmitted through a communication channel assumed to be a Rayleigh fading multipath channel. The mobile radio channel is modeled by using an accepted model [25] consisting of an L tapped-delay-line structure with a tap spacing of one chip and where L corresponds to the number of resolvable multipath. The tap weights α_{kl}, $k = 1, 2, \ldots, D$ and $l = 0, 1, \ldots, L-1$ are assumed to be independent and identically distributed (I.I.D) Rayleigh random variables with a probability density function (PDF) given by [25]

$$f_{\alpha_{kl}}(x) = \frac{2x}{\sigma_f^2}\, e^{-\frac{x^2}{\sigma_f^2}}; \quad x \geq 0 \tag{2}$$

where $E(\alpha_{kl}^2) = \sigma_f^2$ is the fading channel power and the fading phases ψ_{kl} are (I.I.D) random variables uniformly distributed over the interval $[0,\ 2\pi)$. We also assume that the fading amplitude is constant during an observation interval but changes from one observation time to another.

The complex received signal at the mth branch of the array antenna can be expressed as [26]

$$\begin{aligned} r_m(t) \;=\; & \sqrt{2P_R}\left\{\sum_{l=0}^{L-1} \alpha_{1l} C_1(t-\tau_1-lT_c)\, e^{j(w_c t+\emptyset_{1l})} e^{-j\pi(m-1)\sin(\theta_s)}\right\} \\ & +\sqrt{2P_I}\left\{\sum_{k=2}^{D}\sum_{l=0}^{L-1} \alpha_{kl} b_k(t-\tau_k-lT_c) C_k(t-\tau_k-lT_c)\, e^{j(w_c t+\emptyset_{kl})} e^{-j\pi(m-1)\sin(\theta_k)}\right\} + n_{BPm}(t); \\ & m = 1, 2, \ldots, M \end{aligned} \tag{3}$$

where P_R is the average received power of the initial synchronization user, P_I is the average received power of each interfering signal, τ_k the relative time delay associated with the asynchronous communication channel, $\emptyset_{kl} = \varphi_k - \psi_{kl} - w_c(\tau_k + lT_c)$ represents I.I.D random variables uniformly distributed in $[0,\ 2\pi)$, T_c is the chip time duration, θ_s is the direction of arrival (DOA) of the desired user and θ_k is the DOA of the interfering user. Assuming that $(D-1)$ interfering users are engaged in the data transmission, then their corresponding signals are ideally power-controlled and the average received power of each interfering user is P_I. However, for the initial synchronization user, it is not possible to consider ideal power control before successful code acquisition. Hence, the average received power of the initial synchronization user is usually different from that of the data transmission users. This power is denoted by P_R. In Equation (3) the received signal can be divided into three parts, the received signal from the desired user, the multiple access interferences (MAIs) from the $(D-1)$ interfering users and an additive white Gaussian bandpass noise (AWGN) with a double-sided power spectral density of $N_0/2$.

2.2. Statistics of the Correlators Outputs

In this section, we derive the probability density function (PDF) of the in-phase I and quadrature phase Q components at the output of the active correlator for each of the m branches. The following assumptions are used [27, 28]

(1) The search step size is $T_c/2$,
(2) $R \gg 1$ such that the correlation between the received and the locally generated PN sequence is zero when they are not aligned,

(3) The self-interference of the desired user caused by the $(L-1)$ paths, and the multiple access interference MAI caused by the other $(D-1)$ users can be modeled as an additive white Gaussian noise.

The complex equivalent baseband signal $V_m(t)$ at the input of the correlator for the mth element can be written as [26]

$$V_m(t) = \sqrt{P}_R \left\{ \sum_{l=0}^{L-1} \alpha_{1l} C_1 (t - \tau_1 - lT_c) (\cos(\emptyset_{1l}) + j \sin(\emptyset_{1l})) \right\} e^{-j\pi(m-1)\sin(\theta_s)} + \sqrt{P}_I \left\{ \sum_{k=2}^{D} \sum_{l=0}^{L-1} \alpha_{kl} b_k (t - \tau_k - lT_c) C_k (t - \tau_k - lT_c) (\cos(\emptyset_{kl}) + j \sin(\emptyset_{kl})) e^{-j\pi(m-1)\sin(\theta_k)} \right\} + n_m(t); \quad m = 1, 2, \ldots, M \tag{4}$$

where $n_m(t) = n_m^I(t) + jn_m^Q(t)$ is a complex AWGN with mean zero and variance $N_0/2$. The correlator output can then be expressed as

$$Y_m = \underbrace{\left\{ \sum_{l=0}^{L-1} \left(Y_{D,l}^I + jY_{D,l}^Q \right) \right\}}_{1} e^{-j\pi(m-1)\sin(\theta_s)} + \underbrace{\left\{ \sum_{k=2}^{D} \sum_{l=0}^{L-1} \left(Y_{MAI,k,l}^I + jY_{MAI,k,l}^Q \right) e^{-j\pi(m-1)\sin(\theta_k)} \right\}}_{2} + \underbrace{\left\{ N_m^I + jN_m^Q \right\}}_{3}; \quad m = 1, 2, \ldots, M. \tag{5}$$

The in-phase and quadrature phase components of the self-interference (term 1), the multiple access interference (term 2) and thermal noise (term 3) can be modeled as Gaussian random variables with corresponding means and variances given by (A7) to (A13) as shown in Appendix A. These results will be used in the next section to determine the PDF at the output of the LMS processor under the aligned and non-aligned hypotheses.

2.3. Smart Antenna and Adaptive Beamforming

Smart antenna in the proposed system performs beamforming. This operation is achieved by adjusting weights of each of the antenna elements used in the array so that the signals received from all elements are in phase in a particular direction. This will direct the main array pattern towards the desired user and introduces nulls at interfering directions. We use the least mean square (LMS) algorithm which incorporates an iterative procedure that makes successive corrections to the weight vector $\mathbf{W} = [w_1\ w_2\ \ldots\ w_M]^T$ in order to achieve a minimum mean square error ($MMSE$). The LMS algorithm is important because of its simplicity and ease of implementation [12].

The updated weights can be written as

$$w_m(n+1) = w_m(n) + \mu e^*(n) Y_m(n); \quad m = 1, 2, \ldots, M \tag{6}$$

where

$$e(n) = M - \mathbf{W}^H(n)\,\mathbf{Y}(n) \tag{6a}$$

and $\mathbf{Y}(n) = [Y_1(n)\ Y_2(n)\ \ldots\ Y_M(n)]^T$, we choose $\mu = 1/M$ to insure the convergence of the LMS algorithm [12].

When the optimum weight vector $\mathbf{W}$ is obtained and the $MMSE$ is achieved, this vector is used to generate a spatial correlation output z given by [13]

$$z = \mathbf{W^H Y} \tag{7}$$

where $\mathbf{Y} = [Y_1\ Y_2\ \ldots\ Y_M]^T$ are the correlators outputs from the M branches. Equation (5) can be expressed in a vector form as

$$\mathbf{Y} = \left(Y_D^I + jY_D^Q \right) \mathbf{a}(\theta_s) + \sum_{k=2}^{D} \left(Y_{MAI,k}^I + jY_{MAI,k}^Q \right) \mathbf{a}(\theta_k) + \mathbf{N^I} + j\mathbf{N^Q} \tag{8}$$

where

$$Y_D^{I,Q} = \sum_{l=0}^{L-1} \left(Y_{D,l}^{I,Q} \right); \quad Y_{MAI,k}^{I,Q} = \sum_{l=0}^{L-1} Y_{MAI,k,l}^{I,Q} \quad \text{and} \quad \mathbf{N^{I,Q}} = \left[N_1^{I,Q} \; N_2^{I,Q} \; \ldots \; N_M^{I,Q} \right]^T \tag{8a}$$

and

$$\mathbf{a}\left(\theta\right) = \left[1 \quad e^{-j\pi \sin(\theta)} \quad \ldots \quad e^{-j\pi(M-1)\sin(\theta)} \right]^T \tag{8b}$$

is the array steering vector.

Perfect weights are that combine different signals in order to compensate the different phase shifts created by the steering vector at each branch, if we assume that the smart antenna can track perfectly the desired user then

$$\mathbf{W} = \mathbf{a}\left(\theta_s\right) \tag{9}$$

Substituting for $\mathbf{W}$ in (7) and (8) and using $\mathbf{a}(\theta_s)^{\mathbf{H}}\mathbf{a}(\theta_s) = M$, then z can be found to be

$$z = M\left(Y_D^I + jY_D^Q \right) + \sum_{k=2}^{D} \left(Y_{MAI,k}^I + jY_{MAI,k}^Q \right) \mathbf{a}\left(\theta_s\right)^H \mathbf{a}(\theta_k) + \mathbf{a}\left(\theta_s\right)^H \left(\mathbf{N^I} + j\mathbf{N^Q} \right) \tag{10}$$

where

$$\mathbf{a}\left(\theta_s\right)^H \mathbf{a}\left(\theta_k\right) = e^{-j\frac{(M-1)}{2}\psi} \frac{\sin(\frac{M}{2}\psi)}{\sin(\frac{\psi}{2})} \triangleq M \times \mathrm{AF}_n(\theta_k) \tag{10a}$$

$\psi = \pi[\sin(\theta_k) - \sin\left(\theta_s\right)]$ and $\mathrm{AF}_n(\psi)$ is by definition the normalized array factor which represents a pattern function associated with the array geometry. We observe from (10a) that the normalized array factor $|\mathrm{AF}_n(\psi)|$ has a maximum value of 1 in the direction of the desired user, while the other directions of the interfering users are affected by different values smaller than 1. In conclusion by steering the main beam toward the desired user, the smart antennas provide an alternative mean to cope with MAIs by decreasing the total power level of interfering users. Consequently z can be written as

$$z = M\left(Y_D^I + jY_D^Q \right) + M\sum_{k=2}^{D} \left(Y_{MAI,k}^I + jY_{MAI,k}^Q \right) \mathrm{AF}_n\left(\theta_k\right) + \mathbf{a}\left(\theta_s\right)^H \left(\mathbf{N^I} + j\mathbf{N^Q} \right) \tag{11}$$

In addition, the noise components $N_1^{I,Q}, \ldots, N_M^{I,Q}$ are assumed to be independent from one branch to another and thus by exploiting the circular property of complex Gaussian random variables (RVs) the variance of the in-phase thermal noise term in (11) becomes (see Appendix A)

$$E\left(\mathbf{a}\left(\theta_s\right)^{\mathbf{H}} \mathbf{N^I}^H \mathbf{N^I} \mathbf{a}\left(\theta_s\right) \right) = M\frac{1}{2RS_{\text{chip}}} \tag{12}$$

In the case of aligned hypothesis H_1, the in-phase and quadrature-phase components of z are Gaussian random variables with mean zero while the variance can be obtained using (A7), (A8) and (A9) such that

$$E\left[\left(z^I\right)^2 \right] = E\left[\left(z^Q\right)^2 \right] = M^2 \left(\frac{9\sigma_f^2}{32} \right) + M\sigma_0^2 = M\sigma_0^2\left(1 + M\nu\right) \tag{13}$$

where

$$\nu = \frac{9\sigma_f^2}{32\sigma_0^2} \tag{13a}$$

$$\sigma_f^2 = E\left(\alpha_{kl}^2\right) \tag{13b}$$

and

$$\sigma_0^2 = M\left(\frac{\left(L-1\right)\sigma_f^2}{3R} + \frac{L\beta\sum_{k=2}^{D} |\mathrm{AF}_n(\theta_k)|^2 \sigma_f^2}{3R} \right) + \frac{1}{2RS_{\text{chip}}} \tag{13c}$$

It should be noted that σ_0^2 represents the background noise resulting from three signals; namely the self-interference from the non-aligned paths, the multiple access interference caused by interfering users and thermal noise generated at the antenna array. This shows clearly that the MAI term is affected by the beam pattern and this MAI and the self-interference are modeled as a net increase in the noise power.

Given the Gaussian nature of z^I and z^Q, the final decision variable $Z = |z|^2$ is a central chi-square distributed with two degrees of freedom. Its PDF can be expressed as [8]

$$f_{Z|H_1}(z|H_1) = \frac{1}{M2\sigma_0^2(1+M\nu)} \exp\left(\frac{-z}{M2\sigma_0^2(1+M\nu)}\right); \quad z \geq 0 \tag{14}$$

The probability density function of the decision variable Z under hypothesis H_0 can be obtained from Equation (14) to be

$$f_{Z|H_0}(z|H_0) = \frac{1}{M2\sigma_0^2} \exp\left(\frac{-z}{M2\sigma_0^2}\right); \quad z \geq 0 \tag{15}$$

From (14) we can observe that the use of a smart antenna will improve the SNR significantly (maybe a little less than the maximum gain $10\log_{10}(M)$ dB [13]) as compared to a single antenna case.

3. ODV-CFAR AUTOMATIC CENSORING PROCESSOR

In the serial search strategy, the PN code acquisition of DS-CDMA signals is considered as a binary hypothesis testing problem since each cell is classified as one of the two states; H_1 representing a correct phase and H_0 for incorrect phase case. Due to receiving multiple replicas of the transmitted PN codes in multipath fading radio communication environments, usually there exist more than one state H_1, in which the locally generated and the received codes may become synchronous, and hence satisfying the presence of multiple H_1 cells in the reference window (sliding window) used to estimate the background noise level given by (13c) (a contribution of three main terms: thermal noise, MAI interference caused by other users, and the self-interference caused by the nonaligned paths) as shown in Figure 3.

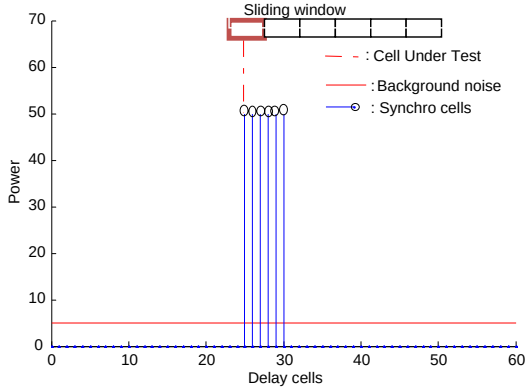

Figure 3. PN acquisition in presence of corrupted cells in the reference window due to multipath.

Based on the assumption that the communication channel is modeled as an L tapped delay line that correspond to the L resolvable multipath. The multipath intensity profile (MIP) is assumed to be either uniform or exponentially decaying with the decay rate μ. When the total fading power in all the resolvable paths is normalized to unity, the average fading power in each resolvable path can be expressed as [29]

$$E\left[\alpha_{kl}^2\right] = \begin{cases} \dfrac{1}{L}; & \mu = 0 \\ \dfrac{1-e^{-\mu}}{1-e^{-\mu L}} e^{-(l-1)\mu}; & \mu \neq 0;\ l = 1, 2, \ldots, L \end{cases} \tag{16}$$

Hence, each resolvable path contributes two (02) H_1 cells because the search step size is $T_c/2$. We note that in real situations the parameter L is not only unknown but can also vary with time. Consequently, if the number of cells to be censored is not properly selected, the system may undergo significant performance degradation. It is well known that the performance of the conventional CA-CFAR detector, which is suboptimum in a homogeneous environment and is equivalent to the optimum Neyman-Pearson detector as the number of reference cells increases, is serious degraded in the presence of multipath. However, to overcome this problem, many alternative CFAR processors have been proposed in the literature, and in particular order statistics (OS) based CFAR processor proved to be more robust [14–21]. In OS-CFAR processing, the references cells are rank ordered in an ascending order according to their magnitude. The higher cells are thus assumed to contain noise plus interference, which may be discarded if the exact number is known as this is not the case in real situations, since they unnecessarily raise the threshold which may cause a serious degradation in the probability of detection. The OS-CFAR processor considered in [4] estimates the background noise power from kth smallest cell in the reference window. In the censored mean level detector (CMLD) CFAR considered in [15, 16] some largest range cells are censored from the reference window and the threshold is computed from the remaining cells. The CMLD is robust against multipath interference as long as the number of censored cells exceeds the number of multipath interference. A generalization of the OS-CFAR and the CMLD known as the trimmed mean TM-CFAR detector has been studied in [1]. All the conventional ordered statistics detectors (OS-CFAR, CMLD and TM-CFAR) have been known to yield good performance as long as the cells containing multipath signals are properly discarded. However, in the previous acquisition systems, the number of censored cells is preset for the radios environments, while in practical situations, the number of corrupted cells depending on the parameter of the model L is not only unknown but can also vary with time as explained earlier. For this reason, we propose to use in an adaptive thresholding scheme for maintaining the probability of false alarm constant while the probability of detection is robust. The most important feature of the proposed system is its ability to dynamically estimate the number of multipath signals that may lie in the reference window by using an automatic iterative backward censoring technique based on ordered data variability (ODV) index. The ODV-CFAR dynamically selects a group of reference cells to use in forming the threshold. This can be summarized as shown in Figure 4.

The decision variables at the output of the square law detector are sent serially in a shift register of length $N_c + 1$. The first cell Z_0 corresponds to the cell under test and the remaining cells correspond

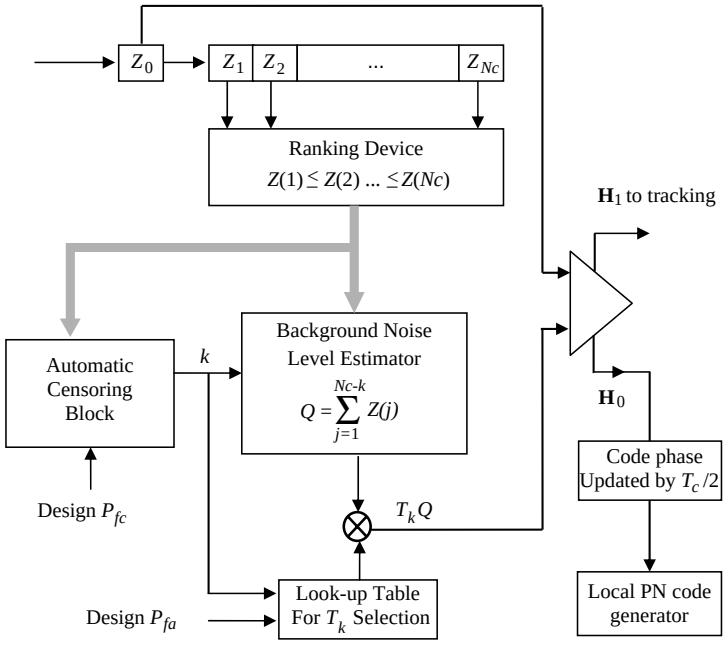

Figure 4. ODV-CFAR automatic censoring processor.

to the reference window which stores the output of the previous code phases. The reference cells are ranked in ascending order according to their magnitude to form the order statistics

$$Z(1) \leq Z(2) \ldots \leq Z(N_c) \tag{17}$$

The indices in parentheses indicate the rank order number, $Z(1)$ and $Z(N_c)$ denote the minimum and the maximum value respectively. Then the unwanted cells are censored, where the number is determined by an automatic censoring block as will be described next in Section 3.1. After censoring the unwanted cells, an estimate of the background noise level is formed from the remaining ordered data cells as

$$Q = \sum_{j=1}^{Nc-k} Z(j) \tag{18}$$

where N_c is the number of reference cells and k is the number of cells censored from the upper end by the censoring block. This estimate is then multiplied by a constant T_k which is selected so that to achieve a desired false alarm probability P_{fa}. Implemented as a look-up table, the threshold multiplier is then used to yield an adaptive threshold T_kQ. Finally, the test cell Z_0 is compared with the adaptive threshold T_kQ in order to make a decision about synchronization according to the following testing hypothesis:

$$Z_0 \underset{H_0}{\overset{H_1}{\gtrless}} T_kQ \tag{19}$$

If the threshold is exceeded, then a correct cell has been found and tracking is performed. Otherwise, the local PN code generator is automatically adjusted to the next offset position, and the test is repeated.

3.1. Description of the Censoring Block Algorithm

The proposed censoring algorithm uses the variability index [18]; it is an iterative backward method which automatically estimates the number of largest samples to be discarded. The basic idea is to consider that the p lowest cells represent the initial estimation of the background noise level, provided that $p \geq 12$, next at each kth step ($k = 0, \ldots, Nc - p - 1$), we form the ordered subset $E_s(k) = [Z(1), Z(2), \ldots, Z(p), Z(Nc-k)]$ and an ODV statistic corresponding to a shape parameter of this population $E_s(k)$ is computed as follows [18]

$$V_k = \frac{\sigma_p + (Z(Nc-k))^2}{(\mu_p + Z(Nc-k))^2} \tag{20}$$

where

$$\mu_p = \sum_{i=0}^{p} Z(i) \quad \text{and} \quad \sigma_p = \sum_{i=0}^{p} [Z(i)]^2 \tag{21}$$

then V_k is compared with a threshold S_k to decide whether the cells used in V_k are from a homogeneous or a nonhomogeneous population using the following test

$$V_k \underset{H_0}{\overset{H_1}{\gtrless}} S_k \tag{22}$$

If H_1 in (22) is true, then the subset $E_s(k) = [Z(1), Z(2), \ldots, Z(p), Z(Nc-k)]$ is assumed to be nonhomogeneous, the ordered statistic $Z(Nc-k)$ is rejected and the test is performed again with k incremented by one. This is continued until the test of (22) is not true that is we have hypothesis H_0 and the censoring algorithm stops. Next, the obtained value of k is used to yield the statistic Q given in (18) by censoring the k highest cells and select the corresponding scaling factor T_k such that P_{fa} is maintained constant at the design value. In each test, the corresponding thresholds S_k are fixed such that a probability of false censoring P_{fc} is maintained. We define this probability representing the probability of test hypothesis error in a homogenous population at the kth step by

$$P_{fc} = \text{Prob}\{V_k > S_k / [Z(1), \ldots, Z(p), Z(N_c - k)] \quad \text{Homogeneous}\} \tag{23}$$

Since an analytic closed expression for the PDF of V_k is not available, we resort to Monte Carlo simulations to estimate P_{fc}. The ODV-based censoring algorithm can be summarized as follows:

Step 1: Set $k = 0$;
Step 2: Form the ordered subset $E_s(k) = [Z(1), Z(2), \ldots, Z(p), Z(Nc-k)]$;
Step 3: Compute the shape parameter V_k of the subset $E_s(k)$;
Step 4: Perform the ODV-based hypothesis test given by (22);
Step 5: If H_1 is a true, repeat steps 2, 3 and 4 for $k = 1, 2, \ldots$ until H_0 is true or $k = N_c - p$;
Step 6: if H_0 is a true, obtain the number of corrupted cells k.

Table 1 gives some values of the parameter S_k computed using Monte Carlo simulations. In practical systems with programmable signal processing capability this values are stored in a look-up table.

Table 1. ODV thresholds for a $P_{fc} = 10^{-2}$ and different size N_c of the reference window.

(Nc, p)	S_k							
	S_0	S_1	S_2	S_3	S_4	S_5	S_6	S_7
(16, 12)	0.356	0.247	0.199	0.173	-	-	-	-
(24, 16)	0.331	0.235	0.190	0.162	0.143	0.131	0.123	0.117

3.2. Performance Analysis of the ODV-CFAR Detector

In the proposed censoring processor, the number of censored cells k is obtained by an automatic censoring block and the remaining ones are used to form the statistic

$$Q = \sum_{j=1}^{Nc-k} Z(j) \tag{24}$$

then the cell under test Z_0 is compared with the adaptive threshold T_kQ in order to make a decision according to the decision rule

$$Z_0 \underset{H_0}{\overset{H_1}{\gtrless}} T_kQ \tag{25}$$

The probability of false alarm in this case is given by

$$P_{fa} = P\{Z_0 > T_kQ/H_0\} = \int_0^{\infty} \int_{T_kQ}^{\infty} f_{Z_0}(Z_0/H_0)\, f_Q(q/H_0)\, dz_0 dq \tag{26}$$

Substituting $f_{Z_0}(z_0/_{H0})$ from (15) into (26), we obtain

$$P_{fa} = \int_0^{\infty} \exp\left(\frac{-T_kq}{M2\sigma_0^2}\right) f_Q(q/H_0)\, dq \triangleq \Phi_Q\left(\frac{T_k}{M2\sigma_0^2}\right) \tag{27}$$

where $\Phi_Q(\cdot)$ denotes the moment generating function (MGF) of Q. Equation (27) will be used to derive a closed form expression for P_{fa} in terms of T_k. As shown in Appendix B, the probability of false alarm P_{fa} is given by [30]

$$P_{fa} = \left\{ \frac{N_c}{(N_c-k)} \left[\frac{1}{1+T_k} - \sum_{m=0}^{k-1} \sum_{j=0}^{N_c-m-1} \binom{N_c-1}{m} \binom{N_c-m-1}{j} (-1)^j \frac{1}{T_k+m+j+1} \right] \right\}^{N_c-k} \tag{28}$$

As a special case, when $k = 0$ (i.e., without censoring) the expression of the P_{fa} is reduced to

$$P_{fa} = \left[\frac{1}{1+T_k}\right]^{N_c} \tag{29}$$

which is just the probability of false alarm of the CA-CFAR processor in a homogenous environment as expected, and which used widely in the literature to determine the scaling factor T_k.

4. SIMULATION RESULTS AND DISCUSSIONS

In this section, we evaluate the performance of the proposed adaptive thresholding acquisition scheme with smart antennas by means of computer simulations for various parameters. To demonstrate the functionality of this communication system, a design probability of false alarm $P_{fa} = 10^{-3}$ is used. The multipath intensity profile (MIP) is assumed to be uniform ($\mu = 0$) (except when it is indicated to have other values) as a result the Rayleigh fading channel power is set to $\sigma_f = 1/L$, and the correlation length integer of the dwell time interval is set at the value of $R = 128$. The adaptive ODV-CFAR thresholding is also compared with other CFAR detectors such as CA-CFAR [1] and OS-CFAR [4] detectors in different situations. For the OS-CFAR processor simulations, the cell representing the threshold is selected equal to $k = 0.75\,Nc$ [31] while the p lowest cells parameter in the OVD-CFAR detector is selected equal to 16. We first assess the capabilities of the ODV-CFAR processor in estimating the mean power level of the background noise used in setting the adaptive threshold. In Figure 5, we show the probabilities of detection P_d as a function of the SNR/chip for the proposed ODV-CFAR and OS-CFAR detectors in the absence of interferences. The optimum Neyman-Pearson (N-P) detector is also presented for comparison purposes. For a number of antenna elements $M = 3$ and in the absence of interferences, we observe that both detectors have comparable probabilities of detection which are almost equal to the probability of detection of the optimum Neyman-Pearson detector. There is a slight improvement for the ODV-CFAR detector over the OS-CFAR detector and some CFAR loss relative to the optimal N-P detector. Note that in the absence of interferences, the proposed system is reduced to CA-CFAR processing, which is known to be an appropriate processor in such a homogeneous background radio environment.

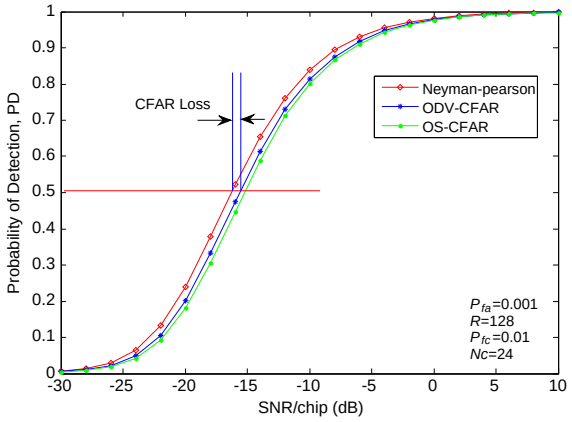

Figure 5. Probabilities of detection of the optimal N-P, ODV-CFAR and OS-CFAR detectors in a homogenous background (no interferences in the reference window); $P_{fa} = 10^{-3}$, $N_c = 24$ and $M = 3$.

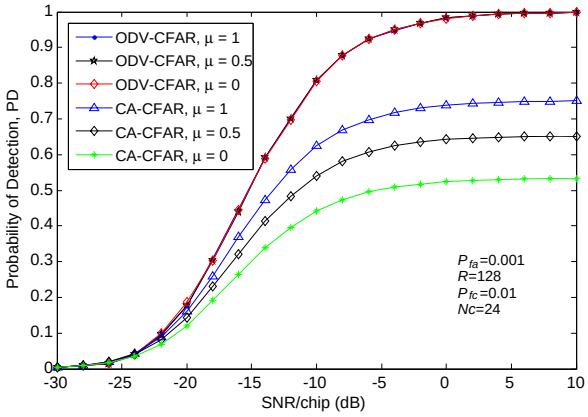

Figure 6. Probabilities of detection of the ODV-CFAR and CA-CFAR detectors with $r = 1$ and the decay rate μ as a parameter; $P_{fa} = 10^{-3}$, $Nc = 24$, $M = 3$.

For a number of antenna elements $M = 3$, Figure 6 shows the effects of μ on the detection probability of the proposed system ODV-CFAR and the CA-CFAR processor in the presence of one interference ($r = 1$) in the reference window. We observe a degradation of the performance of the CA-CFAR processor as the parameter μ decreases. Note that $\mu = 0$ is the worst case situation for a uniform multipath intensity profile. We can also observe that varying μ has no effect on the performance of the ODV-CFAR detector because the interference is successfully removed by the censoring algorithm. This robustness against interference of the proposed algorithm over the CA-CFAR detector is clearly observed which represents a desirable feature in many practical situations.

For the same number of antenna elements $M = 3$ and in the presence of r interferences in the reference window, we observe from Figure 7 that probability of detection of the CA-CFAR processor based on the arithmetic mean of the reference cells is seriously reduced as the number of interferences

increases as expected, while the detection performance of the ODV-CFAR processor based on order statistics of the output references cells and automatic censoring maintains its robustness in the sense that that no excessive degradation of the performance occurs.

As the number of interferences r is further increased to $r = 7$, we now observe from Figure 8 a performance degradation of the OS-CFAR detector even though it is an order statistics based detector, which presents a serious limitation due to the fact that the number of interferences exceeds a known integer threshold which is defined to be $N_c - k$, where $k = 3Nc/4$; that is an interference has been selected for background noise level estimation resulting in an overestimated threshold and thus degradation of the performance.

In Figure 9, we present the detection performance of the ODV-CFAR processor for $r = 3$ interfering signals while the number of antenna elements is increased from $M = 1$ to $M = 6$. We observe that the probability of detection increases as expected. However, the rate of increase decreases with the number of antennas. This enhancement in the detection performance is due to the attractive features of smart antennas in the enhancement of the signal to noise ratio by reducing the power of the noise after

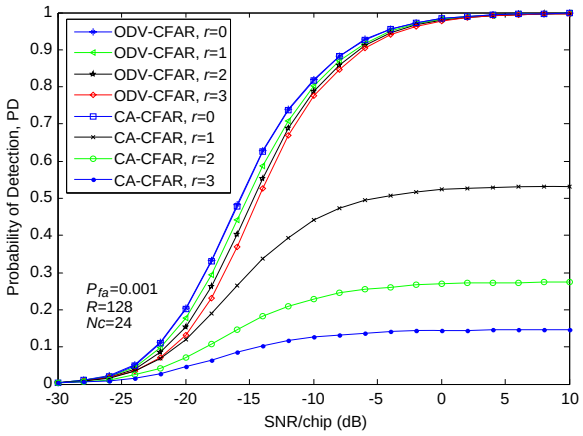

Figure 7. Probabilities of detection of the ODV-CFAR and CA-CFAR detectors with the number of interferences r as a parameter; $P_{fa} = 10^{-3}$, $Nc = 24$, $M = 3$.

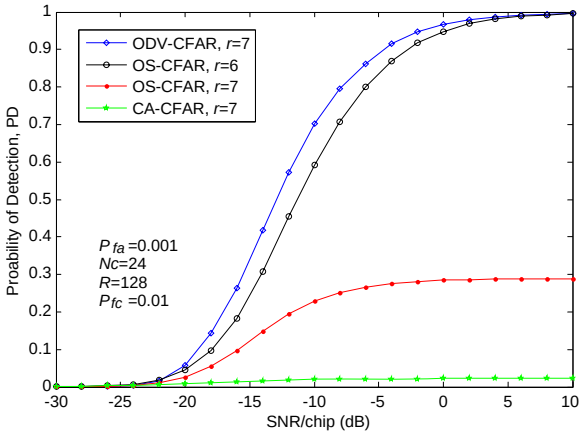

Figure 8. Probabilities of detection of the ODV-CFAR, CA-CFAR and OS-CFAR detectors in the presence of r interferences in the reference window; $P_{fa} = 10^{-3}$, $Nc = 24$, $M = 3$.

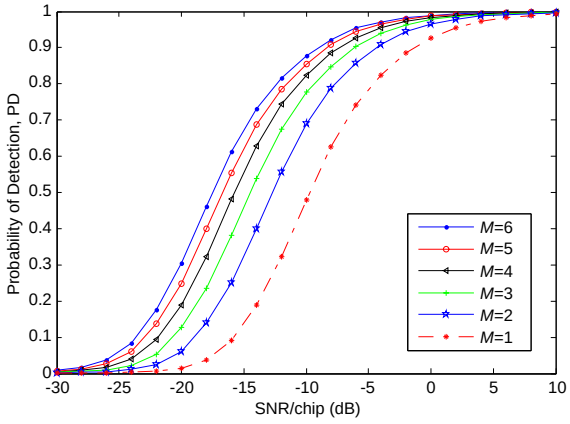

Figure 9. Detection performance of the proposed system with the number of antennas M as a parameter; $P_{fa} = 10^{-3}$, $Nc = 24$ and $r = 3$.

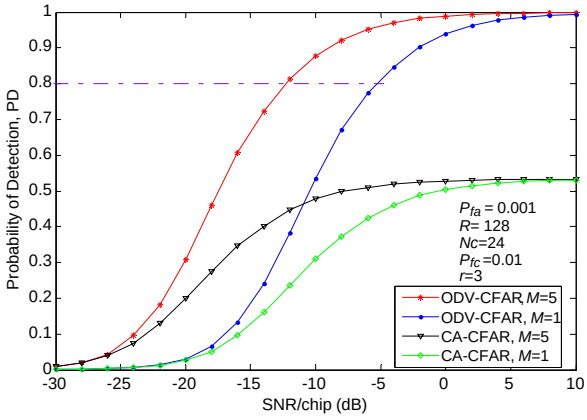

Figure 10. Probability of detection versus SNR/chip of the ODV-CFAR and CA-CFAR processors in the presence of $r = 3$ interferences for different number of antennas M; $P_{fa} = 10^{-3}$ and $Nc = 24$.

the sum of the different branches of the antenna array, and thus consolidating the signal in a specific direction, which is the direction of the interest user. We also observe that when the number of antennas is greater than $M = 4$, we start to reach a saturation level. On other hand, a slight enhancement of performance is attained with a high complexity in the signal processing unit which increases the cost of the hardware implementation.

Figure 10 shows the detection probability without smart-antenna ($M = 1$) and with five elements smart antenna ($M = 5$) while the number of interfering signals is still $r = 3$. These results represent an upper bound of the system performance because this simulation is conducted under the assumption that the LMS weights converge to the optimum weights. In practice, these weights do not match the actual values leading to a slightly reduction in detection performance.

In conclusion, we observe from the simulation results and as expected the use of smart antennas improves the system performance. For example, for a probability of detection $Pd = 0.8$ and with an $M = 5$ antenna elements we have a 6.73 dB improvement in SNR/chip as compared to the single antenna element ($M = 1$) case. Therefore, when an acquisition DS-CDMA employs the proposed PN code acquisition with a smart antenna, any user can transmit a signal with a smaller power than with a single antenna case.

5. CONCLUSION

In this paper, we considered the problem of serial PN code acquisition using smart antennas and adaptive thresholding CFAR based on ordered data variability index. An automatic censoring scheme of an unknown number of interferences samples in Rayleigh fading multipath communication channels was proposed. We called this new censoring CFAR processing ODV-CFAR. The detector employed ordered statistics to determine and censor the unwanted samples in the reference window. A closed form expression for the probability of false alarm was obtained while the performance of the proposed system in terms of the probability of detection was assessed by means of Monte Carlo simulations. The simulation results showed that the adaptive thresholding CFAR scheme proposed with smart antennas enhanced seriously the robustness of PN code acquisition as compared to both the CA-CFAR and OS-CFAR processors in multipath and MAI environments. A drawback, however, is the additional computational load compared to conventional CFAR processors, but with the existence of powerful and high-speed digital signal processors (DSP and FPGA) such computational load increase would not be a major concern. Nevertheless, the simulation results showed that this novel approach of using smart antenna with ODV-CFAR adaptive thresholding was able to produce robust performance regardless of its surrounding environment.

ACKNOWLEDGMENT

The authors are grateful to the anonymous reviewers for their constructive and valuable comments that led to the enhancement of the quality of the paper.

APPENDIX A.

In this appendix, we derive the statistics of the self-interference, the multiple access interference MAI and the thermal noise random variables. The in-phase signal component in (5) due to the user of interest is given by [28]

$$Y_{D,l}^{I} = \frac{\alpha_{1l}\cos\left(\emptyset_{1l}\right)}{RT_c}\left[\Delta_1 R_R\left(j, N+1\right) + \left(T_c - \Delta_1\right)R_R\left(j, N\right)\right] \tag{A1}$$

In Equation (A1), Δ_1 is a random variable uniformly distributed in $[0, T_c]$ and $R_R(j, N)$ is the code partial autocorrelation function of the desired user defined as

$$R_R\left(j, N\right) = \sum_{s=0}^{R-1} C_{1,s+j} C_{1,s+j+N} \tag{A2}$$

The in-phase multiple access interference term can also be expressed as

$$Y^I_{MAI,k,l} = \frac{\sqrt{\beta}\alpha_{kl}\cos(\emptyset_{kl})}{RT_c}\left[\Delta_k R^{(k)}_R(j,N+1) + (T_c - \Delta_k)R^{(k)}_R(j,N)\right] \tag{A3}$$

where $\beta = P_I/P_R$ is the power of the interfering user to the desired signal ratio and $R^{(k)}_R(j,N+1)$ is the partial crosscorrelation between the received sequence and the locally generated code of the desired user, which can be expressed as

$$R^{(k)}_R(j,N) = \sum_{s=0}^{R-1} C_{k,s+j}C_{1,s+j+N} \tag{A4}$$

Finally, the noise term is determined by

$$N^I_m = \frac{1}{\sqrt{P}_R RT_c}\int_0^{RT_c} n^I_m(t)C_1\left(t - j\frac{T_c}{2}\right)dt \tag{A5}$$

The quadrature phase components can be obtained from the in-phase components if we replace $\cos(\cdot)$ by $\sin(\cdot)$ in all the previous equations.

Note that since the acquisition system can acquire only one path at any time, the other $(L-1)$ path signals of the interest user inflict self interference to the aligned path. However, the term of the user of interest can be viewed as

$$\left[Y^I_{D,l} + \sum_{\substack{k=0\\k\neq l}}^{L-1}\left(Y^I_{D,k}\right)\right] = \frac{3}{4}\alpha_{kl}\cos(\emptyset_{kl}) + \sum_{\substack{k=0\\k\neq l}}^{L-1}\left(Y^I_{D,k}\right) \tag{A6}$$

Since α_{kl} are assumed to be independent and identically distributed (I.I.D) Rayleigh random variables with a probability density function (PDF) given by (2) and $\emptyset_{kl}$ are uniformly distributed in [0, 2π), then the first term in (A6) is a Gaussian RV [8] with mean zero and variance equal to

$$E\left[\left(\frac{3}{4}\alpha_{kl}\cos(\emptyset_{kl})\right)^2\right] = \frac{9\sigma_f^2}{32} \tag{A7}$$

From (A1), the second term in (A6) is modelled as a Gaussian random variable with mean zero. We can show that the variance of each element of $(L-1)$ path is

$$E\left[\left(Y^I_{D,l}\right)^2\right] = \frac{\sigma_f^2}{3R} \tag{A8}$$

The multiple access interference term given by (A3) can also be approximated as a Gaussian random variable with zero mean and variance equal to

$$\mathrm{Var}\left(Y^I_{MAI,k,l}\right) = \frac{\beta\sigma_f^2}{3R} \tag{A9}$$

Finally, the in-phase noise component given by (A5) is also a Gaussian random variable with mean zero and variance

$$E\left[\left(N^I_m\right)^2\right] = \frac{1}{2RS_{\text{chip}}} \tag{A10}$$

where $S_{\text{chip}} = P_R T_c/N_0$ represents the signal to noise ratio per chip SNR/chip.

Similarly, the statistics of the quadrature-phase components can also obtained following the above approach.

When the lth resolvable path of the received signal is aligned with the local PN code (Hypothesis H_1), the in-phase and quadrature-phase components of term 1 in Equation (5) are Gaussian RVs with mean zero and variance

$$E\left[\left(\mathrm{Y}^I_{D,l} + \sum_{\substack{k=0\\k\neq l}}^{L-1}\left(Y^I_{D,k}\right)\right)^2\right] = \frac{9\sigma_f^2}{32} + \frac{(L-1)\,\sigma_f^2}{3R} \tag{A11}$$

$Y^I_{MAI,k}$ given by (8a) are Gaussian RVs with mean zero and variance

$$E\left[\left(Y^I_{MAI,k}\right)^2\right] = \frac{L\beta\sigma_f^2}{3R} \tag{A12}$$

The term 3 is also a Gaussian RV with mean zero and variance given by (A10):

$$E\left(N_m^{I^2}\right) = \frac{1}{2RS_{\text{chip}}}; \quad m = 1, 2, \ldots, M. \tag{A13}$$

APPENDIX B.

In this appendix, we present an outline of the proof of Equation (28). A formula relates the threshold multiplier T_k to the desired probability of false alarm P_{fa} after obtaining the appropriate density of Q. For a population of Nc (I.I.D) random variables $\{q_1, q_2, \ldots, q_{Nc}\}$, let $\{Z_1, Z_2, \ldots, Z_{N_c-k}$ be the remaining set of variables upon censoring the k largest samples of $\{q_i;\ i = 1; Nc$. Since q_i are I.I.D., it follows that Z_i, $i = 1, \ldots, N_c - k$ are also I.I.D. From [8], the ith rank ordered random variable has probability density function

$$g_i(z) = \frac{N_c!}{(N_c - i)!\,(i-1)!}\left[F_Z(z)\right]^{i-1}\left[1 - F_Z(z)\right]^{N_c-i} f_Z(z) \tag{B1}$$

where $F_Z(z)$ and $f_Z(z)$ are the cumulative probability distribution and the probability density respectively, common to the I.I.D. Nc random variables prior to ranking given by

$$f_Z(z) = \frac{1}{M2\sigma_0^2}\exp\left(\frac{-z}{M2\sigma_0^2}\right) \quad \text{and} \quad F_Z(z) = 1 - \exp\left(\frac{-z}{M2\sigma_0^2}\right) \tag{B2}$$

Since a particular Z_i is equally likely to have any rank from 1 to $Nc-k$, its probability density function $h_k(z)$ is obtained by averaging (B1) over the uniform distribution of the rank i of Z_i to yield

$$h_k(z) = \frac{1}{N_c - k}\sum_{l=1}^{N_c-k} g_l(z) \tag{B3}$$

Using (B1) and after some mathematical manipulations, we obtain the expression of the common probability density function of $Nc - k$ RVs after censoring k samples as [30]

$$h_k(z) = \frac{N_c}{(N_c - k)} f_Z(z)\left\{1 - \sum_{m=0}^{k-1}\binom{N_c-1}{m} F_z(z)^{N_c-m-1}\left[1 - F_Z(z)\right]^m\right\} \tag{B4}$$

Then using Laplace transform of equation of (B4), the MGF $\Phi_Q(\cdot)$ is found to be

$$\Phi_Q(\omega) = \left\{\frac{N_c}{(N_c-k)}\left[\frac{1}{1+M2\sigma_0^2\omega} - \sum_{m=0}^{k-1}\sum_{j=0}^{N_c-m-1}\binom{N_c-1}{m}\binom{N_c-m-1}{j}(-1)^j\frac{1}{M2\sigma_0^2\omega+m+j+1}\right]\right\}^{N_c-k} \tag{B5}$$

Setting $\omega = T_k/M2\sigma_0^2$ and substituting Equation (B5) in (27) the probability of false alarm is obtained as

$$p_{fa} = \left\{\frac{N_c}{(N_c-k)}\left[\frac{1}{1+T_k} - \sum_{m=0}^{k-1}\sum_{j=0}^{N_c-m-1}\binom{N_c-1}{m}\binom{N_c-m-1}{j}(-1)^j\frac{1}{T_k+m+j+1}\right]\right\}^{N_c-k} \tag{B6}$$

REFERENCES

1. Sofwan, A. and M. Barkat, "PN code acquisition using smart sntennas and adaptive thresholding trimmed-mean CFAR processing for CDMA communication," *Spring World Congress on Engineering and Technology, SCET 2012*, 1–4, China, May 2012.
2. Polydoros, A. and C. L. Weber, "A unified approach to serial search spread-spectrum code acquisition — Part I: General theory," *IEEE Transactions on Communications*, Vol. 32, No. 5, 542–549, May 1984.
3. Linatti, J., "On the threshold setting principles on code acquisition of DS-SS signals," *IEEE Journal on Selected Areas in Communications*, Vol. 18, No. 1, 62–72, Jan. 2000.
4. Kim, C. J., H. J. Lee, and H. S. Lee, "Adaptive acquisition of PN sequences for DSSS communications," *IEEE Transactions on Communications*, Vol. 46, No. 8, 993–996, Aug. 1998.
5. Kim, C. J., "Adaptive acquisition of PN code in multipath fading mobile channels," *Electronics Letters*, Vol. 38, No. 2, 135–137, Jan. 2002.
6. Benkrinah, S. and M. Barkat, "An adaptive acquisition using order statistic CFAR in DS-CDMA serial search for a multipath Rayleigh fading channel," *Proceedings of the Third IEEE International Conference on Systems, Signals and Devices*, Tunisia, 2005.
7. Finn, H. M. and R. S. Johnson, "Adaptive detection mode with threshold control as a function of spatially sampled clutter level estimates," *RCA Review*, Vol. 29, 414–464, Sep. 1968.
8. Barkat, M., *Signal Detection and Estimation*, 2nd Edition, Artech House, Boston, MA, 2005.
9. Kedia, D., "Comparative analysis of peak correlation characteristics of non-orthogonal spreading codes for wireless systems," *International Journal of Distributed and Parallel Systems (IJDPS)*, Vol. 3, No. 3, 63–74, May 2012.
10. Zhang, X., X. Gao, and Z. Wang, "Blind paralind multiuser detection for smart antenna CDMA system over multipath fading channel," *Progress In Electromagnetics Research*, Vol. 89, 23–38, 2009.
11. Godara, L. C., *Smart Antennas*, 1st Edition, CRC Press LLC, New York, NY, 2004.
12. Wang, B. and H. M. Kwon, "PN code acquisition using smart antenna for spread-spectrum wireless communications — Part I," *IEEE Transactions on Vehicular Technology*, Vol. 52, No. 1, 142–149, Jan. 2003.
13. Wang, B. and H. M. Kwon, "PN code acquisition for DS-CDMA systems employing smart antennas — Part II," *IEEE Transactions on Wireless Communications*, Vol. 2, No. 1, 108–117, Jan. 2003.
14. Gandhi, P. P. and S. A. Kassam, "Analysis of CFAR processors in nonhomogeneous background," *IEEE Transactions on Aerospace and Electronic Systems*, Vol. 24, No. 4, 427–445, Jul. 1988.
15. Alhariqi, N., M. Barkat, and A. Sofwan, "Serial PN acquisition using smart antenna and censored mean level CFAR adaptive thresholding for a DS/CDMA mobile communication," *14th IEEE International Conference on High Performance Computing and Communications (HPCC 2012)*, 1193–1198, Liverpool, UK, Jun. 2012.
16. Rickard, J. T. and G. M. Dillard, "Adaptive detection algorithms for multiple-target situations," *IEEE Transactions on Aerospace and Electronic Systems*, Vol. 13, No. 4, 338–343, Jul. 1977.
17. Ritcey, J. A., "Performance analysis of the censored mean-level detector," *IEEE Transactions on Aerospace and Electronic Systems*, Vol. 22, No. 4, 443–454, Jul. 1986.
18. Smith, M. E. and P. K. Varshney, "Intelligent CFAR processor based on data variability," *IEEE Transactions on Aerospace and Electronic Systems*, Vol. 36, No. 3, 837–847, Jul. 2000.
19. Himonas, S. D. and M. Barkat, "Automatic censored CFAR detection for nonhomogeneous environments," *IEEE Transactions on Aerospace and Electronic Systems*, Vol. 28, No. 1, 286–304, Jan. 1992.
20. Barboy, B., A. Lomes, and E. Perkalski, "Cell-averaging CFAR for multiple-target situations," *IEE Proceedings — Radar, Sonar and Navigation*, Vol. 133, No. 2, 176–186, 1986.
21. Barkat, M., S. D. Himonas, and P. K. Varshney, "CFAR detection for multiple target situations," *IEE Proceedings — Radar, Sonar and Navigation*, Vol. 136, No. 5, 193–209, 1989.

22. Prastitis, L. A., J. Frank, and S. D. Himonas, "Automatic censored cell averaging CFAR detector in nonhomogeneous clutter," *1992 International Radar Conference*, 218–221, Brighton, UK, Oct. 1992.
23. Lehtomäki, J., J. Vartiainen, M. J. Juntti, and H. Saarnisaari, "CFAR outlier detection with forward methods," *IEEE Transactions on Signal Processing*, Vol. 55, No. 9, 4702–4706, 2007.
24. Liu, P.-Z. and C.-Z. Han, "Distributed automatic censored cell-averaging CFAR detector," *Acta Automatica Sinica*, Vol. 35, No. 7, 903–910, 2009.
25. Proakis, J. G., *Digital Communications*, 3rd Edition, McGraw-Hill, New York, 1995.
26. Song, Y. S., H. M. Kwon, and B. J. Min, "Computationally efficient smart antennas for CDMA wireless communications," *IEEE Transactions on Vehicular Technology*, Vol. 50, No. 6, 1613–1628, 2001.
27. Buehrer, R. M., *Code Division Multiple Access (CDMA)*, 1st Edition, Morgan & Claypool, Blacksburg, Virginia, US, 2006.
28. Yang, L.-L. and L. Hanzo, "Serial acquisition of DS-CDMA signals in multipath fading mobile channels," *IEEE Transactions on Vehicular Technology*, Vol. 50, No. 2, 617–628, Mar. 2001.
29. Shin, O. S. and K. B. Lee, "Utilization of multipath for spread-spectrum code acquisition in frequency-selective Rayleigh fading channels," *IEEE Transactions on Communication*, Vol. 49, No. 4, 734–743, Apr. 2001.
30. Berbra, K., M. Barkat, and B. Atrouz, "Analysis of the CMLD in K-distributed clutter for fully correlated/uncorrelated texture," *Proceedings of the 1999 International Radar Conference*, Brest, France, May 1999.
31. Rohling, H., "Radar CFAR thresholding in clutter and multiple target situations," *IEEE Transactions on Aerospace and Electronic Systems*, Vol. 19, No. 4, 608–621, Jul. 1983.